International Journal of Environmental Sciences & Natural Resources
ISSN: 2572-1119

Juniper Publishers
key to the Researchers

Research Article
Volume 34 Issue 4 - January 2025
DOI: 10.19080/IJESNR.2025.34.556395

Int J Environ Sci Nat Res

Focal Depths and Mechanisms of Earthquakes in the Western Makran Region: A 30-Years Perspective

M I H Abbasi[1], Ahmed Shah[2,3], Muhammad Hafeez[2]*, Ibrar Khan[2]*, Burhan Ali Khan[1], A A Abid[4], N Ghani Khan[4] and Billel Touati[1]

[1]*School of Earth and Space Sciences, University of Science and Technology of China, China*

[2]*State Key Laboratory of Lithospheric and Environmental Coevolution, University of Science and Technology of China (USTC), China*

[3]*Center of Excellence in Mineralogy, University of Baluchistan, Pakistan*

[4]*Joint Laboratory of Plasma Application Technology, Institute of Advanced Technology, University of Science and Technology of China, China*

Submission: December 24, 2024; **Published:** January 08, 2025

***Corresponding author:** Muhammad Hafeez, State Key Laboratory of Lithospheric and Environmental Coevolution, University of Science and Technology of China (USTC), Hefei 230026, China

Ibrar Khan, State Key Laboratory of Lithospheric and Environmental Coevolution, University of Science and Technology of China (USTC), Hefei 230026, China

Abstract

Situated in the southern regions of Iran and Pakistan, the Makran subduction zone is bound by the Zendan Fault to the west and the Chaman Fault to the east. This region, lying at the complex confluence of the Arabian, Eurasian, and Indian plates, features intricate structural geology and dynamic tectonic activities, characterized by intermediate to deep focus seismicity, where a most common type of faulting is dip-slip, tracing the down going slab of Oceanic plate. This study employs an inversion technique to decode subsurface information, analyzing Teleseismic P-waveforms and their tailing surface reflections, from seismic events between 1990 and 2018. We meticulously selected 67 events in Western Makran, discarding data compromised by various noise types. We relocated the depth and determined the focal mechanism solutions at the 67 shallows to intermediate earthquakes. Through the application of the Kikuchi and Kanamori method, modeling of Teleseismic P-wave and its tailing surface reflections p^P *and* s^P were performed on filtered data to process Inversion mechanism. Our findings illuminate the seismic behavior along the Jiroft fault, revealing intermediate-depth seismic events that penetrate beyond the crustal thickness and extend into the upper mantle. These insights enhance our understanding of the fault dynamics and tectonic stress distribution in the region, contributing to the broader geological knowledge of the Makran subduction zone.

Keywords: Geology; Teleseismic P-waveforms; Earthquakes; Earth's dynamic processes; Lagoonal environment; seismological science

Introduction

The study of earthquake mechanisms has evolved significantly over the late 20th century, with advancements in seismological science providing deeper insights into Earth's dynamic processes. The decoding of seismic waves has become instrumental in unraveling mysteries surrounding source ruptures, subduction zones, and plate tectonics, thus enriching our understanding of fundamental geotectonic phenomena [1,2].

Located at the complex convergence of the Arabian, Eurasian, and Indian plates, the Makran subduction zone, spanning the southwestern part of Pakistan and southeastern Iran, is a region of significant geophysical interest Figure 1.

This area, bounded by the Zendan Fault in the west and the Chaman Fault in the east, has been an active subduction zone since the Late Cretaceous. The subduction of the oceanic Arabian plate beneath the Eurasian continental plate [3-7] which marks the closure of the Neo-Tethys Ocean, evident approximately 20 million years ago, and has continued to influence regional tectonic dynamics [8,9].

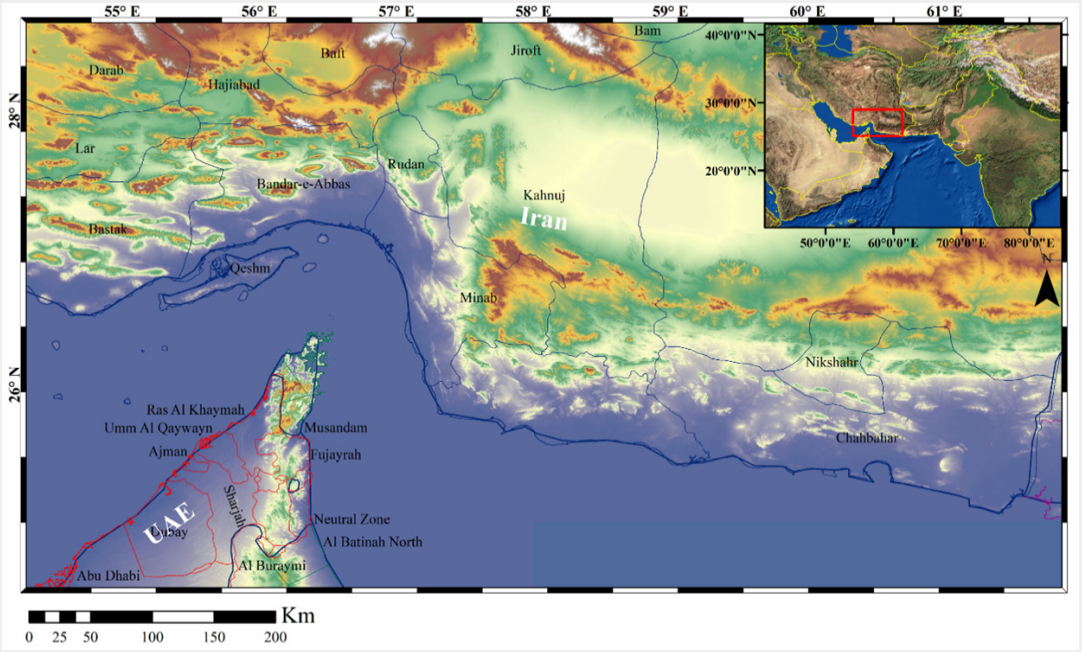

Figure 1: Study area Map, Western Makran.

Makran's proximity to a triple junction, where these major plates (Eurasian, Indian and Arabian) intersect, adds another layer of complexity (Figure 2), [10]. This junction is a hotspot for seismic activity, including some of the largest recorded earthquakes in the region, such as the Mw 8.2 event in 1945 [11].

Despite these significant events, Western Makran often exhibits aseismic behavior, which has been attributed to its high sediment input and low taper, dampening the seismic potential typically expected from such geologically active regions [12].

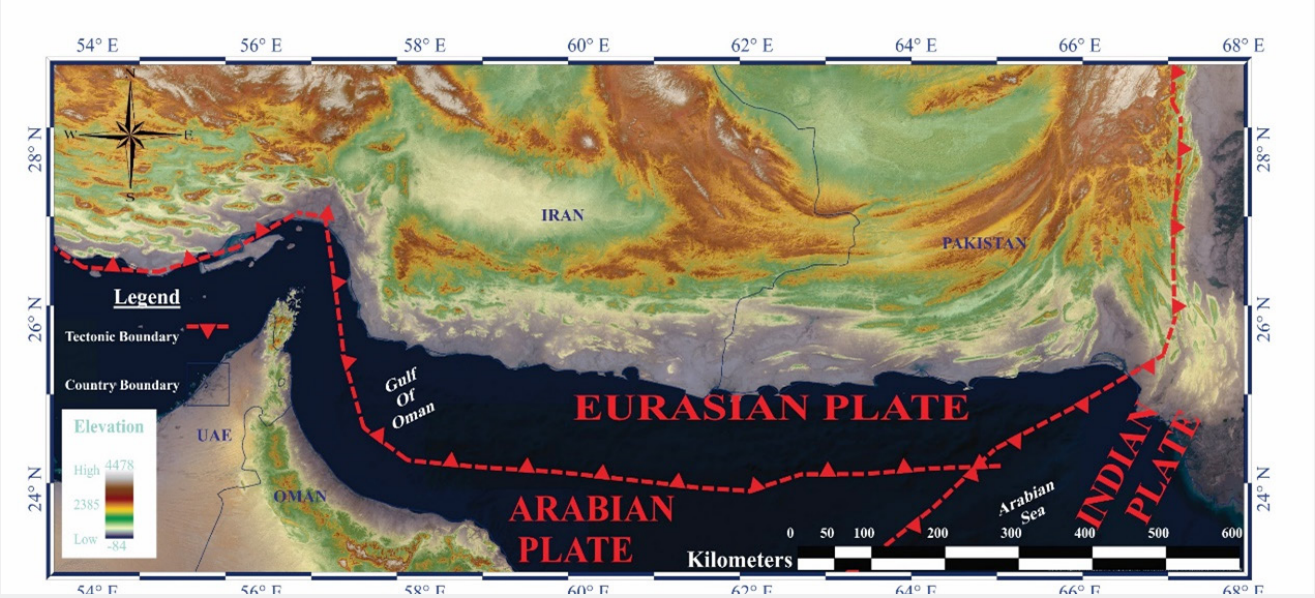

Figure 2: Regional tectonic setting of Makran.

How to cite this article: M I H Abbasi, Ahmed S, Muhammad H, Ibrar K, Burhan Ali K, et al. Focal Depths and Mechanisms of Earthquakes in the Western Makran Region: A 30-Years Perspective. Int J Environ Sci Nat Res. 2025; 34(4): 556395. DOI:10.19080/IJESNR.2025.34.556395

Accretionary wedge related to Makran is said to be World's largest accretionary prism [6,13,14] and extends around 1000km, bounded between Minab-Zindan Fault System (MZFS) is a Dextral fault in Iran and Chaman-Ornach-Nal Fault System (COFS) is a Sinistral fault in Pakistan [7]. The growth of such large Accretionary wedge/prism is believed to be because of deposition and deformation of marine flysch deposit [15] as Makran Accretionary wedge has highest sediments input and highest incoming sediment thickness as well [6] and the wedge is progradation towards sea by trench fill sediments (Kopp et al., 2000).

Recent studies have proposed that the Makran region functions as a separate microplate, defined by distinctive seismic patterns and structural boundaries [5,16]. This characterization is crucial for understanding the seismic risks and geotectonic dynamics of the region, particularly in light of its development significance with projects like the Gwadar and Chabahar ports. Makran is typically a region bounded by Faults from almost all sides and is considered as scrappy part of the Neo-Tethys [5]. Towards west of Makran, it is bounded by of Right lateral MZFS strike-slip fault in Iran [6] and towards eastern side of Makran it has been bounded by Left lateral COFS strike-slip fault, [5]. In Western Makran it is bounded from North by Jiroft Fault (ophiolites) and extending eastwards, towards south this region is bounded by Makran Subduction Thrust in Oman trench which lies ahead of Murray Ridge, which was rifted, is NE-SW trending ridge System and marking the extreme North extension of the Owen Fracture Zone [17]. Currently, sea-floor spreading has a pace of 2mm/a [18], while Owen Fracture Zone (OFZ) is inferred as Transform marginal boundary between Arabian and Indian plates, was in South of OFZ Carlsberg Ridge is terminating in transform boundary [19,20].

Makran has been divided into four subparts from North to South, it extends cross-strike 400±600km from offshore Oman trench to Volcanic arc and ophiolites [13] on basis of Tectono-stratigraphy its divisions are as follow.

The uppermost or northern area of Makran (known as North Makran) is surrounded by the Quaternary deposits of Jaz Murian Depression (JMD) in the region of Iran (in North of Western Makran) and the equivalent Mashkel depression in Pakistan [21-23]. These deposits are mainly composed of metamorphic bodies, continental "terranes" and terrigenous turbidites [10,24] with their sedimentary cover [7]. Ophiolitic sequence, volcanic presence [25,26] imbricates in several lithologies found thrusting southwards on Bajgan-Durkan Complex [27] delineating lower marginal boundary of North Makran (Burg, 2018). Normal faults which are steeply dipping, marking contacts with JMD in Iran and Mashkel forearc basin in Pakistan, near Makran magmatic arcs Chaghi, Rah Kos [28]. Inner Makran mainly composed of marine deposits, lithologies containing sandstones, pelagic red limestones, radiolarian mudstone, shale and terrigenous turbidities, while having thrust sheets between Bashakerd Thrust at Northern part and towards southern part is marked by Ghasr Ghand Thrust [29,30].

Outer Makran lies between Ghasr Ghand Thrust GGT and Chah Khan thrust CKT have Marls, Calcareous sandstones, shales and deep marine turbiditic sequence, deep-sea fan [31,32]. Costal Makran lies among Thrusts Chah Khan thrust CKT towards North and at South current coastal line [33] transitional facies, marl, calcareous sandstones are dominated for several kilometers, Mudstone dominated sequence coarsening up, along with mollusc shells [32] gypsiferous mudstones having mud cracks showing Lagoonal environment in past. Younger successions consist of fluvial sediments and lateral thick beds of continental conglomerates [34].

Figure 3, illustrates the spatial distribution of seismic events recorded in the Western Makran region, highlighting earthquake occurrences with magnitudes ranging from 4.0Mw to 7.8Mw. The map shows a dense cluster of seismicity aligned along major geological features, providing insights into the active tectonic processes in this area. These events are primarily concentrated along the MZFS and the Jiroft Fault, as delineated by the yellow lines. The distribution pattern suggests a significant level of tectonic activity along these fault zones, which are critical in accommodating the northward convergence of the Arabian plate into the Eurasian plate. MZFS, is a major strike-slip fault represents a significant tectonic boundary where stress accumulation and release occur, as evidenced by the clustering of seismic events along this line. The concentration of earthquakes along these faults highlights their role as major conduits for seismic energy release in the Western Makran region. The spatial distribution of these seismic events provides valuable information for assessing the seismic hazard associated with these faults, particularly in relation to the potential for larger earthquakes that can impact the densely populated regions nearby.

Figure 4, presents the spatial distribution of seismic events within the Western Makran region, illustrating both the depth and magnitude of these events in relation to significant tectonic boundaries. The color-coded circles represent the depth at which each earthquake occurred, while the size of each circle indicates the magnitude range of the event. The variation in earthquake depths and magnitudes across different parts of the fault zones can help infer the mechanical properties of the Earth's crust and mantle interactions in these regions.

Material and Methods

For this study, seismic data were acquired from the Seismic Monitoring Agency (IRIS), formatted in Time Series SEED Data format, which is particularly suited for handling high-resolution earthquake data (Goldstein and Snoke, 2005). Table 1 presents a detailed catalog of seismic activities, comprising key parameters and attributes integral to our seismic analysis. Each listed event includes geographical coordinates (latitude and longitude), seismic orientations (strike, dip, rake), chronological data (date and time of occurrence), along with magnitude and depth.

How to cite this article: M I H Abbasi, Ahmed S, Muhammad H, Ibrar K, Burhan Ali K, et al. Focal Depths and Mechanisms of Earthquakes in the Western Makran Region: A 30-Years Perspective. Int J Environ Sci Nat Res. 2025; 34(4): 556395. DOI:10.19080/IJESNR.2025.34.556395

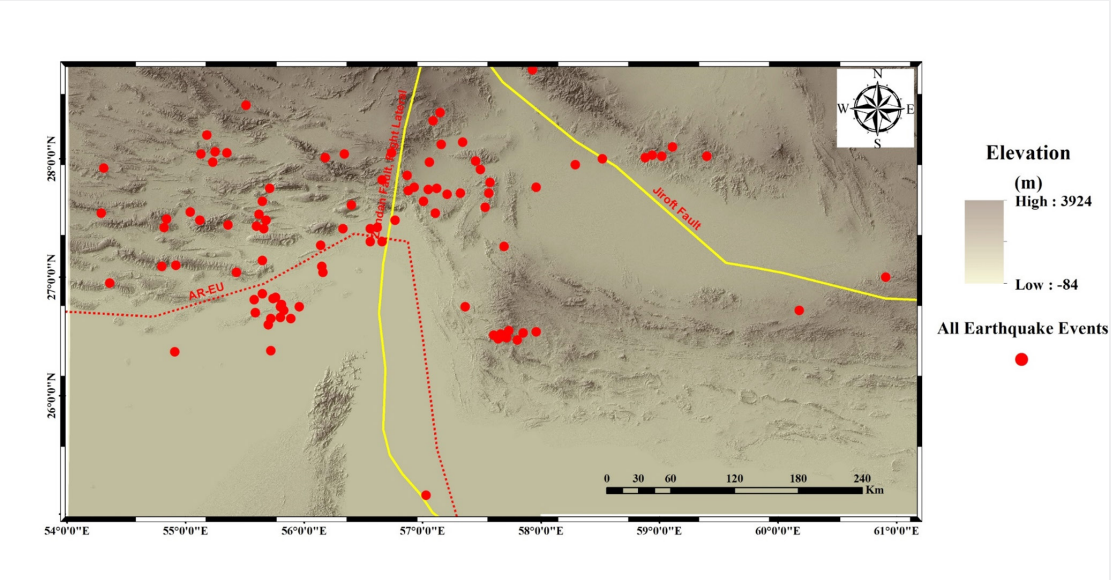

Figure 3: All earthquake events recorded in this area in range of 4.0Mw to 7.8Mw Magnitude.

Table 1: Earthquake data events used in this research.

S. No	Latitude	Longitude	Strike	Dip	Rake	Day of Occurrence (yr m d)	Origin Time (hr m s)	Magnitude	Depth
1	28.06	55.25	274	37	107	19901106	18:45:54	6.2	25
2	27.04	55.43	98	47	66	19910522	16:29:02	5.7	23
3	28.05	55.35	254	40	99	19920519	12:24:57	5.7	33
4	28.45	55.51	110	26	120	19930709	10.29:22	5.2	23
5	28.32	57.09	315	7	125	19960226	8:08:19	5.3	33
6	27.26	57.69	289	21	83	19961018	9:26:03	5.4	33
7	27.64	57.01	215	58	22	19970419	5:53:14	5.5	27
8	27.3	56.56	88	42	92	19980801	23:38:32	5.1	33
9	27.91	57.49	250	16	68	19990304	5:38:28	6.2	33
10	27.61	56.4	290	45	106	20000305	9:40:06	5.6	40.9
11	27.74	57.05	299	32	125	20011125	21:30:55	5.1	40.2
12	27.3	56.66	237	39	36	20020417	8:47:23	5.3	33
13	27.48	56.77	288	18	97	20030214	10:28:59	5.3	37.7
14	27	60.91	97	45	-65	20030624	6:52:52	5.3	61
15	27.59	57.53	102	48	7	20030706	16:04:21	4.9	33
16	26.75	57.36	27	59	161	20040128	9:06:49	5.2	25.7
17	28.75	57.93	280	75	4	20041006	11:14:34	5.1	72.1
18	28.14	57.34	211	67	-156	20041007	12:55:02	5.3	66.5
19	26.66	55.8	257	39	83	20051127	10:22:20	6.1	10
20	26.7	55.59	254	49	52	20051127	11:33:10	5.2	10
21	26.65	55.89	218	87	-2	20051127	16:30:38	5.4	10
22	27.86	56.87	302	19	118	20060228	7:31:03	5.8	18
23	27.43	55.6	269	28	83	20060325	7:28:58	5.7	18

How to cite this article: M I H Abbasi, Ahmed S, Muhammad H, Ibrar K, Burhan Ali K, et al. Focal Depths and Mechanisms of Earthquakes in the Western Makran Region: A 30-Years Perspective. Int J Environ Sci Nat Res. 2025; 34(4): 556395. DOI:10.19080/IJESNR.2025.34.556395

24	27.48	55.68	276	35	89	20060325	9:55:13	5.3	10
25	26.72	55.83	111	45	112	20060603	7:15:35	5.4	12.1
26	27.53	55.62	261	33	59	20060325	11:02:58	5	15
27	26.77	55.81	247	33	96	20060628	21:02:09	5.8	10
28	26.07	61.23	107	67	-12	20060718	23:27:06	5.2	43.8
29	27.97	55.23	280	42	108	20070227	22:28:12	4.5	6
30	27.48	55.12	265	42	69	20070323	21:38:02	4.8	14
31	28.04	56.34	282	34	94	20070425	4:19:02	5.1	16
32	27.14	55.65	270	21	81	20070724	10:08:06	4.6	14
33	28.05	56.74	314	85	-178	20070825	4:24:22	5	10
34	26.65	55.72	234	33	76	20080910	11:00:34	6.1	12
35	26.75	55.96	245	45	59	20080917	17:43:49	5.3	4
36	26.37	54.91	249	31	45	20081025	20:17:20	5.2	28.8
37	26.82	55.74	69	41	115	20081207	13:36:21	5.7	15
38	26.83	55.76	238	49	59	20081208	14:41:43	5.5	6.1
39	26.75	55.8	241	33	73	20081209	15:09:23	5.2	14.1
40	25.16	57.03	227	26	82	20090507	22:44:04	5.4	38.6
41	26.6	55.7	297	44	91	20090722	3:53:03	5.5	9.6
42	27.04	56.16	246	30	63	20091103	23:26:52	5.1	14.1
43	28.1	59.11	36	87	180	20101220	18:41:59	6.1	12
44	28.01	58.88	122	64	-29	20110127	7:02:03	5	10
45	28.03	58.94	133	74	-14	20110128	4:20:36	5	15
46	28.12	57.16	327	5	144	20110305	20:42:54	5.2	19.3
47	27.71	57.56	333	45	157	20110615	1:05:31	5.4	34
48	27.76	57.96	76	54	-164	20120418	17:40:40	5.1	73
49	26.55	57.73	346	74	-178	20130511	2:08:08	5.9	15
50	26.53	57.85	249	78	2	20130511	3:09:47	5.3	8.9
51	26.47	57.8	69	84	5	20130511	18:06:14	4.7	25
52	26.52	57.66	350	63	176	20130512	0:06:59	5.5	17.6
53	26.5	57.68	344	72	179	20130518	10:03:16	5.5	15
54	26.49	57.64	351	69	178	20130518	10:57:47	5.5	15
55	26.51	57.6	352	78	-172	20140202	14:26:45	5.3	10
56	26.38	55.72	112	70	-178	20140527	5:44:30	5.1	14.3
57	27.54	57.11	345	38	138	20140722	15:22:40	5.1	10
58	27.75	55.71	349	41	180	20141110	13:52:27	5.4	10
59	26.12	61.23	308	83	4	20150504	11:30:35	4.8	10
60	28.2	55.18	89	42	113	20160122	20:51:47	5.1	19.5
61	27.41	56.33	233	42	29	20160706	23:58:27	5.1	16
62	27.73	56.88	98	45	151	20170831	1:30:28	5.2	10
63	27.76	56.93	103	45	157	20171023	0:24:14	5.3	10
64	27.8	57.57	313	45	121	20180307	14:46:14	5.2	35.5
65	27.42	56.62	143	43	-74	20180321	20:41:21	5	10
66	27.42	54.82	294	45	85	20180722	5:07:03	5.4	8
67	28.02	59.4	114	65	-10	20180907	6:23:39	5.6	10

How to cite this article: M I H Abbasi, Ahmed S, Muhammad H, Ibrar K, Burhan Ali K, et al. Focal Depths and Mechanisms of Earthquakes in the Western Makran Region: A 30-Years Perspective. Int J Environ Sci Nat Res. 2025; 34(4): 556395. DOI:10.19080/IJESNR.2025.34.556395

To mitigate the impact of noise such as shallow mantle triplications, the epicentral distances of the recording stations were maintained between 30° and 90° for vertical components. This range helps in optimizing the signal-to-noise ratio (S/N) and ensuring the reliability of the seismic data interpretation. The earthquake catalog was enriched with detailed event characteristics from the Global Centroid Moment Tensor (GCMT) database [35]. This database provides comprehensive seismic moment tensors, which are crucial for understanding the source mechanisms of earthquakes.

The Seismic Analysis Code (SAC) software was utilized to process the seismic data. SAC tools enabled us to inspect the data meticulously, pick seismic phases accurately, and enhance S/R, which is pivotal for the detailed analysis of seismic events [36]. These processes ensure the extraction of meaningful seismic signals from the background noise, facilitating robust seismic interpretation.

The numerical method developed by [37] was employed for the direct inversion of complex Teleseismic body waves. This technique involved correlating observed P-waveforms with synthetic waveforms to decipher the subsurface seismic information accurately. The synthetic waveforms were generated using a layered velocity and density model based on CRUST1.0 [38]. This model incorporates five distinct layers, providing a detailed structural representation of the Earth's crust, which is essential for precise seismic wave simulation.

Results and Discussion

Our study's comprehensive analysis of seismic activity in Western Makran has employed advanced seismic inversion techniques to decode subsurface information. Through the application of MATLAB utilities and SAC software, we processed seismic waveform data to extract detailed focal mechanism solutions. These solutions are depicted in the "Beach Ball" diagrams which provide a visual interpretation of stress orientations and fault movement at the moment of seismic events. The localization of seismic events is a critical step in our analysis. We utilized a software-based method incorporating the CRUST1.0 global crustal model, which provides a 1D velocity model at 1x1 degrees resolution. This approach, integrated with MATLAB's built-in scripts, allowed for precise depth relocation and correlation with synthetic waveform data. The resulting alignments and misfits between observed and synthetic data significantly aid in validating the seismic mechanisms inferred from our analysis. Table 2 delineates the outcomes of depth relocation analyses, presenting a comparison of original and relocated depths for selected seismic events alongside the associated misfit values.

Table 2: Depth relocation of events and their misfits.

S. No	Events	Original Depth	Relocated Depth	Misfit
1	19901106	25	12	0.83
2	19910522	23	30	0.57
3	19920519	33	44	0.91
4	19930709	23	8	0.25
5	19960226	33	34	0.81
6	19961018	33	30	0.89
7	19970419	27	24	0.85
8	19980801	33	9	0.94
9	19990304	33	31	0.88
10	20000305	40.9	12	0.85
11	20011125	40.2	10	0.63
12	20020417	33	61	0.65
13	20030214	37.7	56	0.88
14	20030624	61	55	0.95
15	20030706	33	52	0.67
16	20040128	25.7	20	0.38
17	20041006	72.1	72.5	0.59
18	20041007	66.5	85.5	0.58
19	2005112710	10	15	0.9
20	2005112711	10	16	0.62
21	2005112716	10	19	0.84
22	20060228	18	18	0.95

How to cite this article: M I H Abbasi, Ahmed S, Muhammad H, Ibrar K, Burhan Ali K, et al. Focal Depths and Mechanisms of Earthquakes in the Western Makran Region: A 30-Years Perspective. Int J Environ Sci Nat Res. 2025; 34(4): 556395. DOI:10.19080/IJESNR.2025.34.556395

23	2006032507	18	11	0.76
24	2006032509	10	18	0.88
25	20060603	12.1	3	0.66
26	2006032511	15	15	0.91
27	20060628	10	10	0.87
28	20060718	43.8	44	0.84
29	20070227	6	2	0.45
30	20070323	14	12	0.7
31	20070425	16	22	0.68
32	20070724	14	11	0.39
33	20070825	10	3	0.9
34	20080910	12	15	0.92
35	20080917	4	8	0.3
36	20081025	28.8	19	0.8
37	20081207	15	8	0.36
38	20081208	6.1	18	0.77
39	20081209	14.1	6	0.97
40	20090507	38.6	32	0.71
41	20090722	9.6	10	0.74
42	20091103	14.1	15	0.77
43	20101220	12	4	0.97
44	20110127	10	10	0.99
45	20110128	15	15	0.73
46	20110305	19.3	23	0.57
47	20110615	34	23	0.85
48	20120418	73	73	0.67
49	2013051102	15	14	0.96
50	2013051103	8.9	13	0.89
51	2013051118	25	24	0.99
52	20130512	17.6	18	0.79
53	2013051809	15	15	0.9
54	2013051810	15	21	0.77
55	20140202	10	18	0.72
56	20140527	14.3	14	0.93
57	20140722	10	11	0.55
58	20141110	10	18	0.84
59	20150504	10	10	0.87
60	20160122	19.5	30	0.96
61	20160706	16	26	0.79
62	20170831	10	15	0.78
63	20171023	10	10	0.47
64	20180307	35.5	43.5	0.7
65	20180321	10	12	0.65
66	20180722	8	9	0.65
67	20180907	10	11	0.85

How to cite this article: M I H Abbasi, Ahmed S, Muhammad H, Ibrar K, Burhan Ali K, et al. Focal Depths and Mechanisms of Earthquakes in the Western Makran Region: A 30-Years Perspective. Int J Environ Sci Nat Res. 2025; 34(4): 556395. DOI:10.19080/IJESNR.2025.34.556395

Event 1993 07 09 (Figure 5): This event occurred at a depth of 39.0km and showed significant waveform alignments at depths ranging from 38 to 40km, with a minimum misfit observed at 38km. The focal mechanism solution indicates a predominantly dip-slip movement, suggesting a vertically oriented stress regime likely driven by subduction dynamics.

Event 2004 01 28 (Figure 6): Recorded at a depth of 20.0km, this event displayed optimal waveform matching at depths from 10 to 30km. The focal mechanism points to complex faulting with a mix of strike-slip and dip-slip components, reflective of the intricate tectonic interactions at shallower depths within the subduction zone.

Event 2014 07 22 (Figure 7): This shallower event at 11.0km depth presented waveform correlations extending slightly deeper, with best fits around 10 to 12km. The "Beach Ball" diagram suggests a significant strike-slip component, indicative of lateral tectonic movements adjacent to or within the fracture zones.

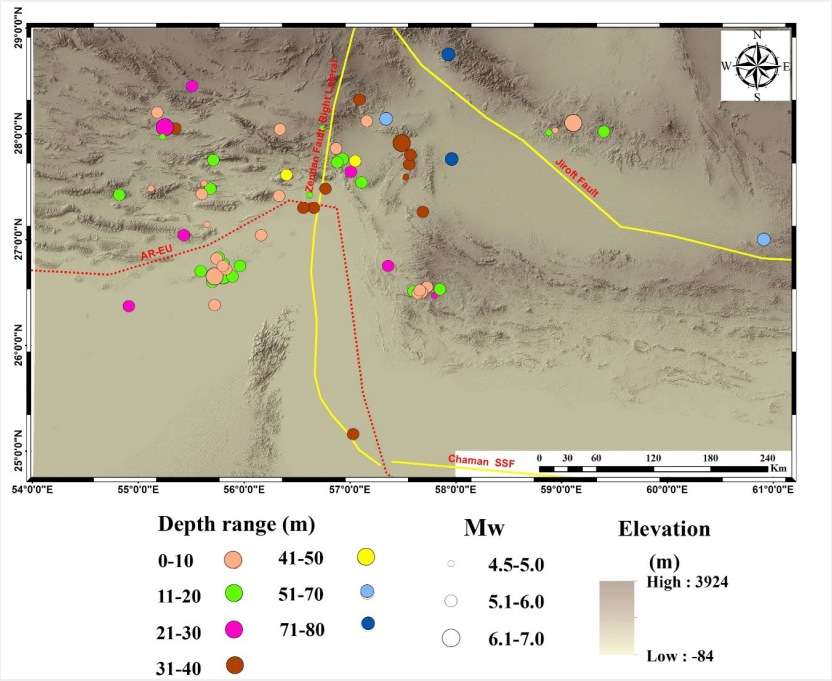

Figure 4: Earthquake events selected for processing along with Depth and Magnitude.

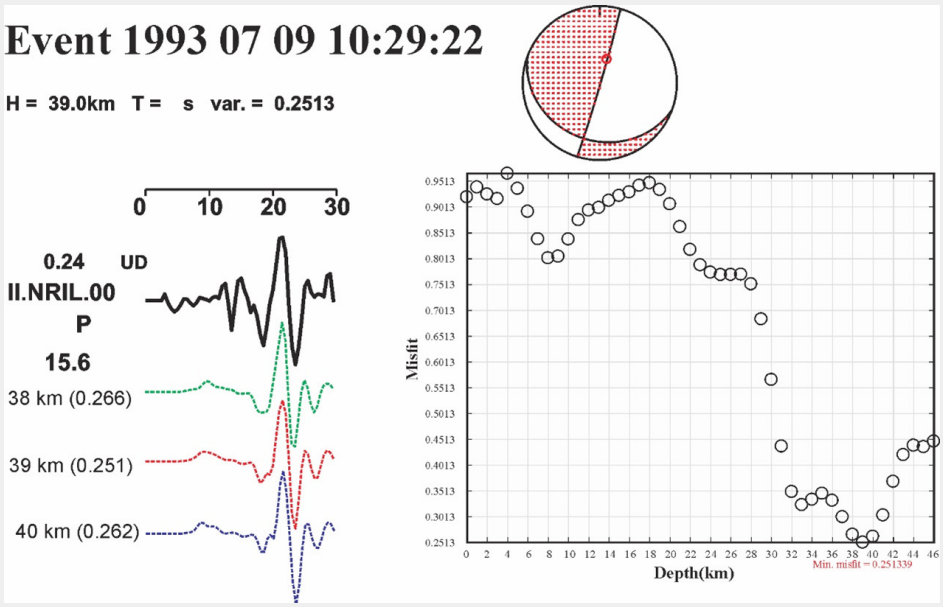

Figure 5: Synthetic waveforms correlated with earthquake event 1990 7 09 10:29:22 for depth relocation.

How to cite this article: M I H Abbasi, Ahmed S, Muhammad H, Ibrar K, Burhan Ali K, et al. Focal Depths and Mechanisms of Earthquakes in the Western Makran Region: A 30-Years Perspective. Int J Environ Sci Nat Res. 2025; 34(4): 556395. DOI:10.19080/IJESNR.2025.34.556395

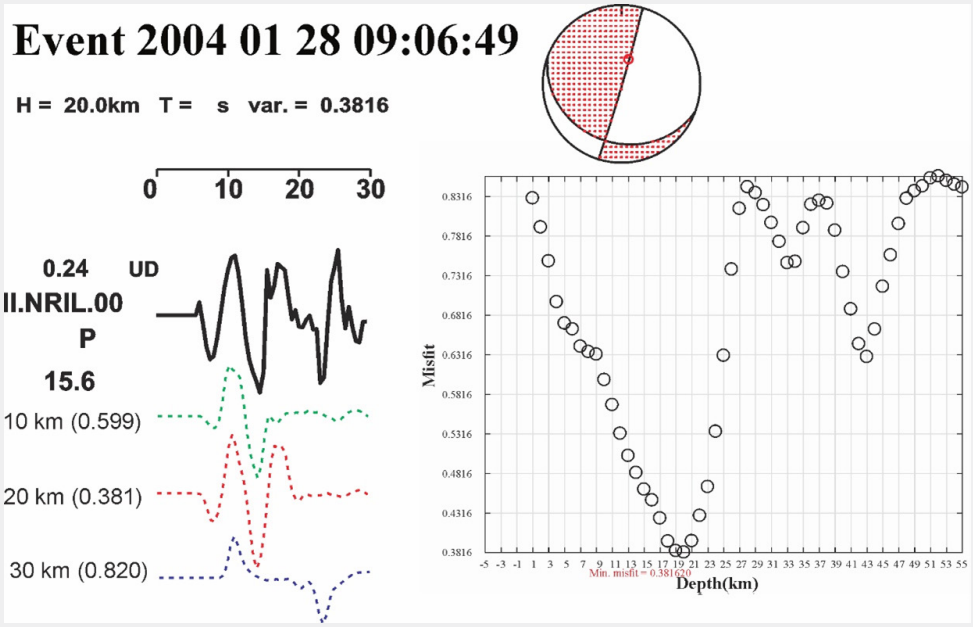

Figure 6: Synthetic waveforms correlated with earthquake event 2004 01 28 09:06:49 for depth relocation.

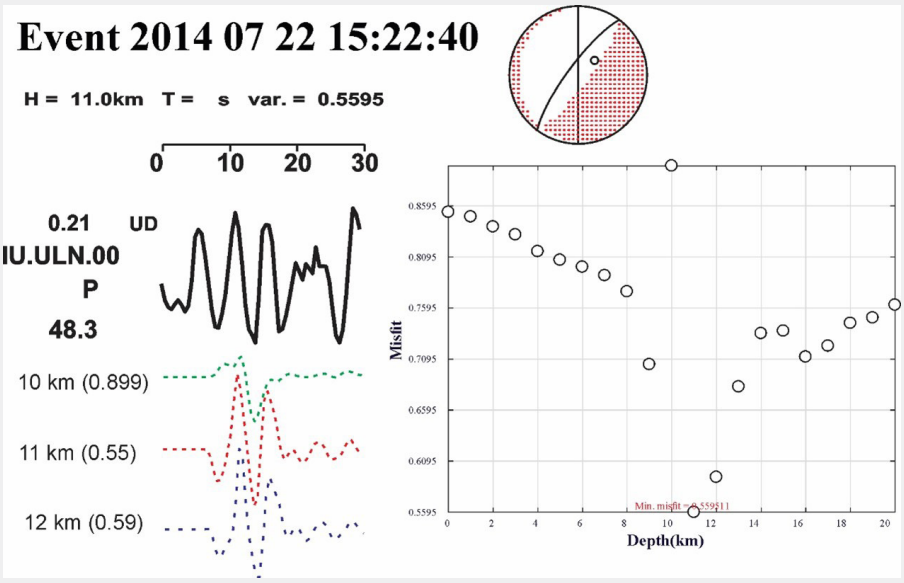

Figure 7: Synthetic waveforms correlated with earthquake event 2014 07 22 15:22:09 for depth relocation.

Figure 8, provides a comprehensive overview of the spatial distribution of seismic events within the Western Makran region, aligned along three strategic cross-sectional profiles: P1, P2, and P3. Each profile is designed to traverse key geological features and fault zones, offering insights into the depth, magnitude, and nature of seismic activity related to the complex tectonic framework of this area

Profile P1 starting from northeast to southwest, this profile captures seismic events across varying depths and magnitudes, illustrating the interaction between tectonic forces at the Eurasian and Arabian plate boundaries. The profile helps in understanding the vertical and lateral extent of seismicity associated with major fault systems, including the strike-slip and reverse fault movements that dominate this region Figure 9. This profile is strategically aligned perpendicular to the Makran subduction complex, offering a unique cross-sectional view of the subduction interface. The Moho shows a progressive descent from the continental side towards the oceanic side, which is characteristic of subduction zones where one tectonic plate slides beneath another.

How to cite this article: M I H Abbasi, Ahmed S, Muhammad H, Ibrar K, Burhan Ali K, et al. Focal Depths and Mechanisms of Earthquakes in the Western Makran Region: A 30-Years Perspective. Int J Environ Sci Nat Res. 2025; 34(4): 556395. DOI:10.19080/IJESNR.2025.34.556395

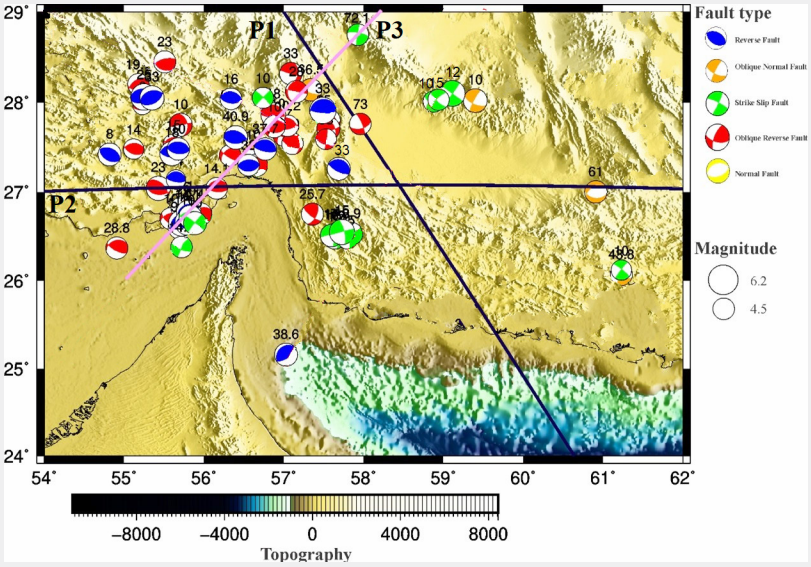

Figure 8: Three Profiles were carried out for cross-sectional view, showing beach ball diagrams along with original respective original depths.

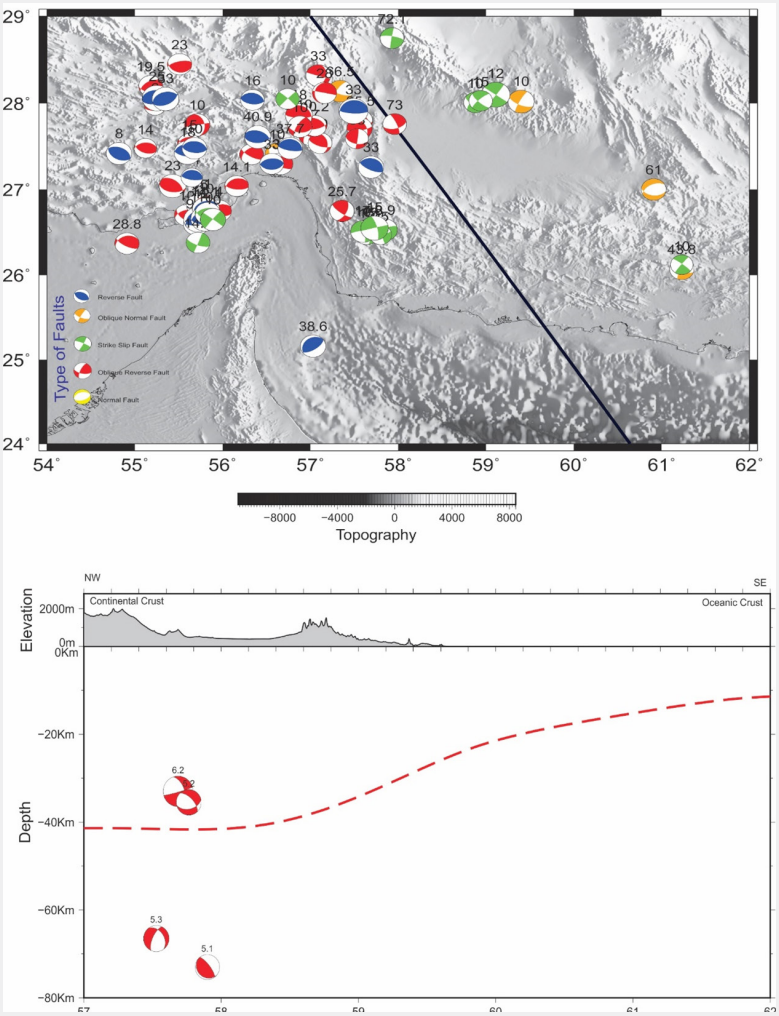

Figure 9: Profile 1 is heading from NW 57° Longitude and 29° Latitude, passing from Continental Crust of Eurasian plate and Arabian Crust. Depicting variation in Mantle from 40kms NW to 11Kms SE.

How to cite this article: M I H Abbasi, Ahmed S, Muhammad H, Ibrar K, Burhan Ali K, et al. Focal Depths and Mechanisms of Earthquakes in the Western Makran Region: A 30-Years Perspective. Int J Environ Sci Nat Res. 2025; 34(4): 556395. DOI:10.19080/IJESNR.2025.34.556395

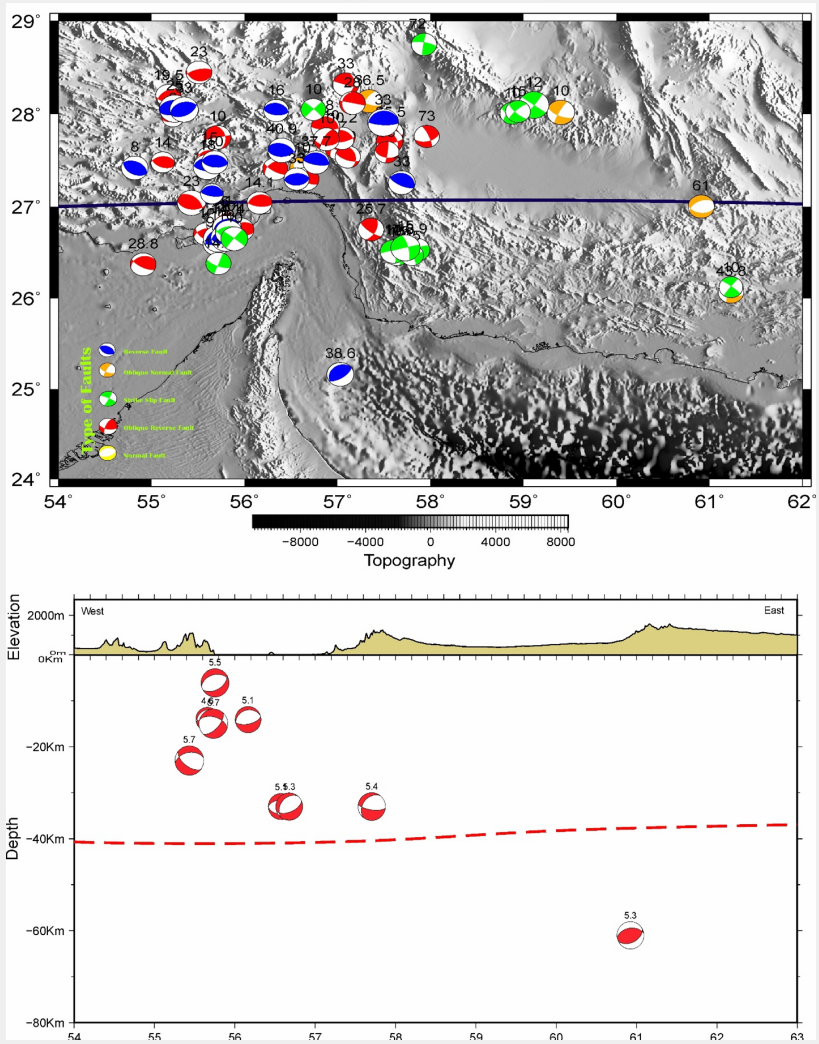

Figure 10: Profile 2, drawn on Latitude 27 ° WE. Moho is almost same along with this profile 40kms deep in West to 37km deep in East of this profile.

The focal mechanisms represented in the "Beach Ball" diagrams indicate a variety of faulting behaviors. The presence of reverse faults, oblique normal faults, and strike-slip faults in this profile illustrates the complex stress regime in this area. These faulting patterns are indicative of the tectonic forces at play, where the oceanic crust is being forced under the continental crust, generating significant seismic activity.

This profile is instrumental in understanding the interaction between the continental crust of the Eurasian plate and the oceanic crust of the Arabian plate. The red dashed line represents the Moho boundary, providing a critical marker for the transition between the crust and the mantle. Observations from this profile indicate a significant depth variation in the Moho, descending from approximately 41km in the continental region to about 11km in the oceanic region. This variation in Moho depth is essential for understanding the dynamics of subduction, as it suggests a steep angle of oceanic plate subduction beneath the continental plate, which is typical of active subduction zones. The cross-section shows a distinct pattern of earthquakes occurring along the subduction zone, where the Arabian oceanic plate is being forced under the Eurasian continental plate. The concentration of deeper and high-magnitude earthquakes near the Zendan Fault (as highlighted by the seismic events near the NW start of the profile) provides evidence of intense tectonic activity and stress accumulation within this region.

Events like the 5.1 magnitude earthquake at a depth of approximately 70km reflect deeper subduction processes, while shallower events may relate to crustal adjustments or sedimentary processes associated with the accretionary wedge.

The occurrence of deep earthquakes can be indicative of the temperature and mechanical strength of the subducting slab. Cooler, more brittle slabs are capable of sustaining the stresses needed to generate earthquakes at greater depths. At certain pressures and temperatures corresponding to depths around 70km and greater, the oceanic crust and upper mantle materials

How to cite this article: M I H Abbasi, Ahmed S, Muhammad H, Ibrar K, Burhan Ali K, et al. Focal Depths and Mechanisms of Earthquakes in the Western Makran Region: A 30-Years Perspective. Int J Environ Sci Nat Res. 2025; 34(4): 556395. DOI:10.19080/IJESNR.2025.34.556395

can undergo mineral phase changes that increase the density and may lead to stress accumulation and subsequent seismic events. At certain pressures and temperatures corresponding to depths around 70km and greater, the oceanic crust and upper mantle materials can undergo mineral phase changes that increase the density and may lead to stress accumulation and subsequent seismic events.

Profile P2 reveals a notable variation in the Moho depth, illustrating the transition from thicker continental crust to thinner oceanic crust as it moves from northwest to southeast. This profile extends from NW at 54° Longitude and 29° Latitude to SE at 69° Longitude and 22° Latitude, spanning a diverse range of topographical features from the elevated continental regions to the lower oceanic terrains Figure 10. The surface elevation profile underscores the transition from rugged, mountainous terrain to the smoother, oceanic seabed, highlighting the geological complexity of the Makran subduction zone. The detailed mapping of seismic events along this profile, particularly that penetrating the Moho and reaching into the mantle, offers insights into the ongoing subduction process. Depth changes in the Moho along this profile reflect the dynamics of subduction, with the depth decreasing from approximately 40km in the NW to almost 37km depths towards the SE.

Profile P3 The depicted seismic events, ranging from shallow to deep (up to 70km), align with both the MZFS and Jiroft faults. The distribution of these events indicates active faulting across a range of depths, with the Jiroft fault exhibiting significant deep seismicity that suggests penetration into the upper mantle Figure 11. This deep seismic activity could be indicative of crustal deformations that extend beyond the crust, emphasizing the dynamic nature of these fault zones.

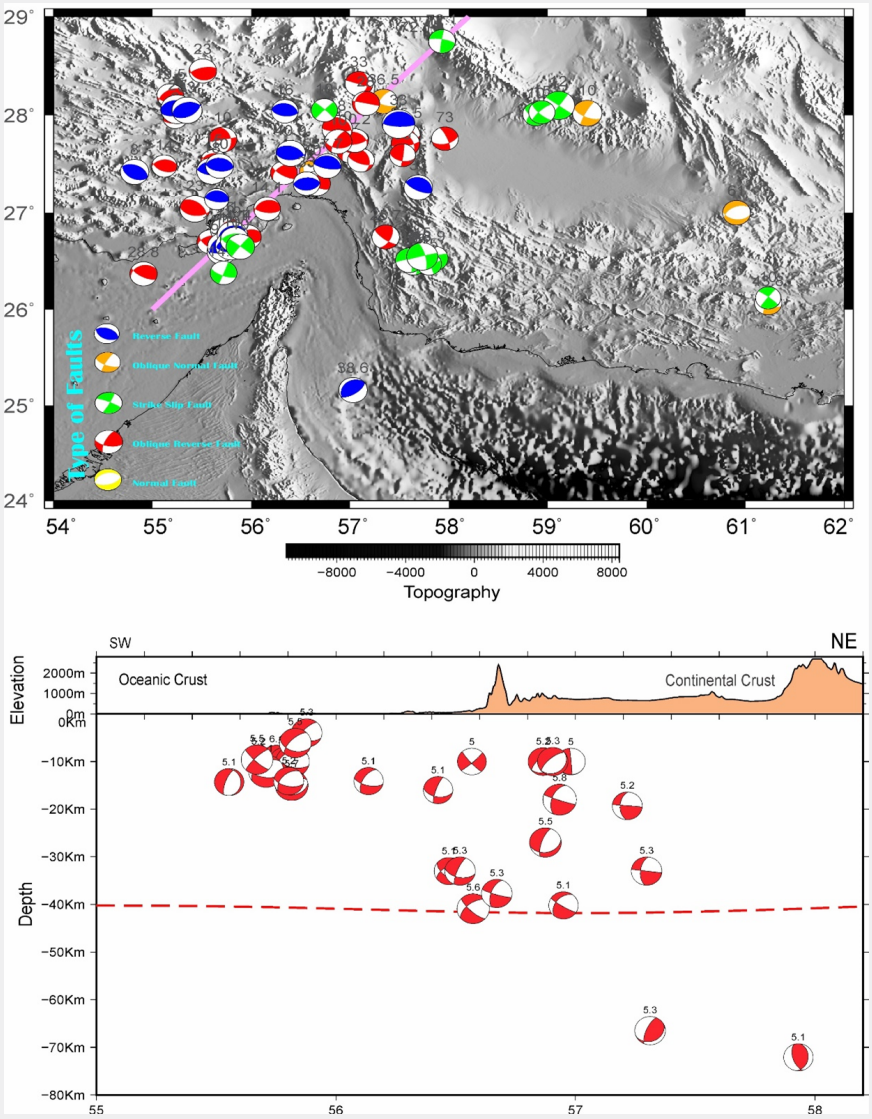

Figure 11: Profile three, covering perpendicular section along Western boundary of Makran, near Bandar Abbas port.

How to cite this article: M I H Abbasi, Ahmed S, Muhammad H, Ibrar K, Burhan Ali K, et al. Focal Depths and Mechanisms of Earthquakes in the Western Makran Region: A 30-Years Perspective. Int J Environ Sci Nat Res. 2025; 34(4): 556395. DOI:10.19080/IJESNR.2025.34.556395

The Moho depth appears relatively uniform across this profile, with minor fluctuations indicating a stable but possibly thinning subduction zone beneath this part of the Makran.

The concentration of earthquakes along this profile, particularly near known fault zones, highlights regions of potential hazard and suggests that these faults are actively accommodating regional tectonic stresses. The presence of deep earthquakes near the Jiroft fault, often associated with a normal faulting mechanism, may suggest the existence of tensional forces at depth, which could be related to the complex dynamics of plate interactions in this area.

Conclusion

This study has systematically documented seismic events that transcend the traditional bounds of crustal thickness, revealing profound tectonic activity along the proposed margins of the Pakistan-Iran Makran Microplate (P-IMM). Notably, these events cluster around the Jiroft Fault, which delineates the northern boundary of the P-IMM adjacent to the Jaz Murian Depression. This fault's trajectory extends eastward into the heart of the Makran Accretionary Prism, with recorded seismicity reaching depths of 60 to 80km. Such profound depths of seismic activity underscore the complex and dynamic nature of this tectonic setting.

Additionally, the Zendan Fault in Iran and the Ornach–Nal Fault in Pakistan form the western and eastern peripheries of the P-IMM, respectively. The southern demarcation aligns with the subduction interface along the Arabian Plate at the Oman Trench. The presence of deep seismic events along these boundaries further supports the hypothesis of the P-IMM as a potentially isolated tectonic entity. This isolation is suggested by the distinct tectonic behaviors and the deep-reaching seismic events that effectively sever this microplate from the surrounding continental structures.

The implications of these findings are significant, suggesting that the P-IMM could represent a unique tectonic entity, distinguished by its deep sub-surface seismic activity and clearly demarcated fault lines that penetrate down to the Moho discontinuity. Such characteristics could indicate a degree of tectonic isolation or a distinct mechanical behavior from the adjoining Eurasian and Arabian plates.

The potential isolation of the P-IMM, if further substantiated, could have significant implications for regional tectonic models and earthquake hazard assessments in the Pakistan-Iran transboundary region. Given the active seismicity and the strategic tectonic setting, continued geophysical monitoring and detailed seismic profiling are recommended to better understand the fault mechanics and potential seismic risks. Such studies are essential for developing more accurate models of earthquake generation and propagation in this tectonically active region.

Statements and Declaration

Ethical Approval: This manuscript has not been published elsewhere in part or in entirety and is not under consideration by another journal. We have read and understood your journal's policies, and we believe that neither the manuscript nor the study violates any of these. We have not submitted our manuscript to a preprint server before submitting it here.

References

1. Banghar AR, Sykes LR (1969) Focal mechanisms of earthquakes in the Indian Ocean and adjacent regions. Journal of Geophysical Research 74(2): 632-649.
2. Shimizu K, Yagi Y, Okuwaki R, Fukahata Y (2019) Development of an inversion method to extract information on fault geometry from teleseismic data. Geophysical Journal International 220(2): 1055-1065.
3. Romano D, Matteucci F (2007) Contrasting copper evolution in ω Centauri and the Milky Way. Monthly Notices of the Royal Astronomical Society: Letters 378(1): L59-L63.
4. DeMets C, Gordon RG, Argus DF (2010) Geologically current plate motions. Geophysical Journal International 181(1): 1-80.
5. Siddiqui NK, Jadoon IAK (2012) Indo-Eurasian Plate collision and the evolution of Pak-Iran Makran Microplate, Pishin-Katawaz Fault Block and the Porali Trough, in Search and Discovery Article# 30265 (2013), PAPG/SPE Annual Technical Conference, 3–5 December 2012, Islamabad, Pakistan.
6. Smith G, McNeill L, Henstock TJ, Bull J (2012) The structure and fault activity of the Makran accretionary prism. Journal of Geophysical Research: Solid Earth 117(B7).
7. Burg JP (2018) Geology of the onshore Makran accretionary wedge: Synthesis and tectonic interpretation. Earth-Science Reviews 185: 1210-1231.
8. Reilinger R, McClusky S, Vernant P, Lawrence S, Ergintav S, et al. (2006) GPS constraints on continental deformation in the Africa-Arabia-Eurasia continental collision zone and implications for the dynamics of plate interactions. Journal of Geophysical Research. Solid Earth 111.
9. Barber DE, Stockli DF, Horton BK, Koshnaw RI (2018) Cenozoic Exhumation and Foreland Basin Evolution of the Zagros Orogen During the Arabia-Eurasia Collision, Western Iran. Tectonics 37(12): 4396-4420.
10. Ellouz-Zimmermann N, Lallemant SJ, Castilla R, Mouchot N, Leturmy P, et al. (2007) Offshore frontal part of the Makran Accretionary prism: The Chamak survey (Pakistan). In: Thrust belts and foreland basins, Springer, pp. 351-366.
11. Pacheco JF, Sykes LR (1992) Seismic moment catalog of large shallow earthquakes, 1900 to 1989. Bulletin of the Seismological Society of America 82(3): 1306-1349.
12. Byrne DE, Davis DM, Sykes LR (1988) Loci and maximum size of thrust earthquakes and the mechanics of the shallow region of subduction zones. Tectonics 7(4): 833-857.
13. Kopp C, Fruehn J, Flueh ER, Reichert C, Kukowski N, et al. (2000) Structure of the Makran subduction zone from wide-angle and reflection seismic data. Tectonophysics 329(1-4): 171-191.
14. Gutscher MA, Westbrook GK (2009) Great earthquakes in slow-subduction, low-taper margins. In: Subduction Zone Geodynamics, Springer, pp. 119-133.

How to cite this article: M I H Abbasi, Ahmed S, Muhammad H, Ibrar K, Burhan Ali K, et al. Focal Depths and Mechanisms of Earthquakes in the Western Makran Region: A 30-Years Perspective. Int J Environ Sci Nat Res. 2025; 34(4): 556395. DOI:10.19080/IJESNR.2025.34.556395

15. Burg JP (2011) The Asia–Kohistan–India collision: review and discussion. In: Arc-continent collision. Springer, pp. 279-309.

16. Abbasi MIH (2020) Is Makran a Separate Microplate? A Short Review. Malaysian Journal of Geosciences (MJG) 5(1): 1-5.

17. Gaedicke C, Schlüter HU, Roeser HA, Prexl A, Schreckenberger B, et al. (2002) Origin of the northern Indus Fan and Murray Ridge, Northern Arabian Sea: interpretation from seismic and magnetic imaging. Tectonophysics 355(1-4): 127-143.

18. DeMets C, Gordon RG, Argus DF, Stein S (1990) Current plate motions. Geophysical journal international 101(2): 425-478.

19. Edwards RA, Minshull TA, White RS (2000) Extension across the Indian–Arabian plate boundary: the Murray Ridge. Geophysical Journal International 142(2): 461-477.

20. Khan M, Liu Y, Farid A, Ahmed H (2019) Indications of uplift from seismic stratigraphy and backstripping of the well data in western Indus offshore Pakistan. Geological Journal 5(1): 553-570.

21. McCall GJH (1985) Explanatory Text of the Minab Quadrangle Map, 1: 250,000. Geological Survey of Iran.

22. Glennie KW, Clarke MWH, Boeuf MGA, Pilaar WFH, Reinhardt BM (1990) Inter-relationship of Makran-Oman Mountains belts of convergence. Geological Society, London, Special Publications 49: 773-786.

23. Dolati A, Burg JP (2013) Preliminary fault analysis and paleostress evolution in the Makran Fold-and-Thrust Belt in Iran, in Lithosphere Dynamics and Sedimentary Basins: The Arabian Plate and Analogues, Springer, pp. 261-277.

24. McCall GJH (1997) The geotectonic history of the Makran and adjacent areas of southern Iran. Journal of Asian Earth Sciences 15(6): 517-531.

25. McCall GJH (2002) A summary of the geology of the Iranian Makran. Geological Society, London, Special Publications, 195: 147-204.

26. Jafari MK, Babaie HA, Moslempour ME (2017) Mid-ocean-ridge to suprasubduction geochemical transition in the hypabyssal and extrusive sequences of major Upper Cretaceous ophiolites of Iran: Tectonic Evolution, Collision, and Seismicity of Southwest Asia. In Honor of Manuel Berberian's Forty-Five Years of Research Contributions 525: 229.

27. McCall GJH, Kidd RGW, Leggett JK (1982) Trench-Forearc Geology: Sedimentation and Tectonics on Modern and Ancient Active Plate Margins.

28. Burg JP, Dolati A, Bernoulli D, Smit J (2013) Structural style of the Makran Tertiary accretionary complex in SE-Iran. In: Lithosphere dynamics and sedimentary basins: The Arabian Plate and analogues, Springer, pp. 239-259.

29. McCall GJH, Eftekhar-Nezad J (1993) Explanatory Text of the Nikhshahr Quadrangle Map, 1: 250 000, L14. Geological Survey of Iran, Tehran.

30. Haghipour N, Burg JP, Kober F, Zeilinger G, Ivy-Ochs S, et al. (2012) Rate of crustal shortening and non-Coulomb behaviour of an active accretionary wedge: The folded fluvial terraces in Makran (SE, Iran). Earth and Planetary Science Letters 355-356: 187-198.

31. Harms JC, Cappel HN, Francis DC (1982) Geology and petroleum potential of the Makran Coast, Pakistan. Society of Petroleum Engineers.

32. Dolati A (2010) Stratigraphy, structural geology and low-temperature thermochronology across the Makran accretionary wedge in Iran.

33. Mohammadi A, Burg JP, Winkler W, Ruh J, von Quadt A (2016) Detrital zircon and provenance analysis of Late Cretaceous–Miocene onshore Iranian Makran strata: Implications for the tectonic setting. GSA Bulletin 128(9-10): 1481-1499.

34. Haghipour N, Burg JP, Ivy-Ochs S, Hajdas I, Kubik P, et al. (2015) Correlation of fluvial terraces and temporal steady-state incision on the onshore Makran accretionary wedge in southeastern Iran: Insight from channel profiles and 10Be exposure dating of strath terraces. GSA Bulletin 127(3-4): 560-583.

35. Ekström G, Nettles M, Dziewoński AM (2012) The global CMT project 2004–2010: Centroid-moment tensors for 13,017 earthquakes. Physics of the Earth and Planetary Interiors 200-201: 1-9.

36. Goldstein P, Snoke A (2005) SAC availability for the IRIS community: Incorporated Research Institutions for Seismology Newsletter, v. 7.

37. Kikuchi M, Kanamori H (1982) Inversion of complex body waves. Bulletin of the Seismological Society of America 72(2): 491-506.

38. Laske G, Masters G, Ma Z, Pasyanos M (2013) Update on CRUST1. 0—A 1-degree global model of Earth's crust. In: Geophys Res Abstr, EGU General Assembly Vienna, Austria, 15: 2658.

DOI: 10.19080/IJESNR.2025.34.556395

How to cite this article: M I H Abbasi, Ahmed S, Muhammad H, Ibrar K, Burhan Ali K, et al. Focal Depths and Mechanisms of Earthquakes in the Western Makran Region: A 30-Years Perspective. Int J Environ Sci Nat Res. 2025; 34(4): 556395. DOI:10.19080/IJESNR.2025.34.556395